Int J Adv Manuf Technol (2007) 32: 1125–1133
DOI 10.1007/s00170-006-0432-7

ORIGINAL ARTICLE

K. Manonmani · N. Murugan · G. Buvanasekaran

Effects of process parameters on the bead geometry of laser beam butt welded stainless steel sheets

Received: 26 April 2005 / Accepted: 3 December 2005 / Published online: 19 April 2006

Abstract Laser beam welding (LBW) is a field of growing importance in industry with respect to traditional welding methodologies due to lower dimension and shape distortion of components and greater processing velocity. Because of its high weld strength to weld size ratio, reliability and minimal heat affected zone, laser welding has become important for varied industrial applications. With increased use of laser welding in continuous mode, there will be increased dependence on the use of equations to predict the dimensions of the weld bead. In this paper, the development of mathematical equations using a three factor 5- level factorial technique to predict the geometry of weld bead in butt joint of austenitic stainless steel 304 sheet of 2.5 mm thickness are presented. The models developed have been checked for their significance by using F-test and t-test. The direct and interaction effect of the process variables on bead geometry are presented in graphical form for quick analysis.

Keywords Laser beam welding · Central composite design · Regression Analysis · SS 304

1 Introduction

Laser beam welding (LBW) is a fusion joining process that uses the energy from a laser beam to melt and subsequently crystallize a metal, resulting in a bond between parts. Lasers generate light energy that can be absorbed into materials and converted to heat energy. Because of high power density of the laser beam, laser welding is characterized by very narrow fusion zone, narrow weld width and high penetration [1]. The energy input in laser welding is controlled by the combination of focused spot size, focused position, shielding gas, laser beam power and welding speed. For the laser beam welding of butt joint, the parameters of joint fit-up and the laser beam to joint alignment [2] becomes important. In applying thermal energy to small areas, there are no other methods as efficient as lasers. Laser welding can be used successfully for welding low carbon, alloy steels, stainless steels, Titanium and its alloys and some Nickel alloys. Specific applications of laser welding include welding of pipeline, shipbuilding, and making micro-connections in electronic industries.

AISI type 304 stainless steels have many advantages such as low thermal conductivity, high resistance to corrosion and high stability at elevated temperatures and also it is a superior absorber of laser light. Due to these advantages, it is used in numerous industries, including electronics, medical instruments, home appliances, automotive and specialized tube industry. The rapid heating and cooling characteristic of laser welding alters the behaviour of stainless steels as compared to its reaction to welding processes with higher heat inputs [3]. A common problem with conventionally welded stainless steel is sensitization, where the residual carbon combines with chromium, reducing the alloys' corrosion resistance. This needs a thorough understanding of the process characteristics affecting the technological and metallurgical characteristics of the weld. The effects of process parameters on bead geometry can be studied with the help of developing mathematical models that can extend the discrete experimental results into a functional relationship that predicts bead quality at all points in the experimental range with estimable accuracy. Such mathematical models are essential for the laser beam welding of stainless steel sheets from which bead geometry, which influences the quality of welded joints, can be predicted. Such models have been developed and reported in the literature. Response surface

K. Manonmani (✉)
Faculty of Mechanical Engineering Department,
Govt. College of Technology,
Coimbatore, Tamilnadu, India
e-mail: manokmani@yahoo.co.in

N. Murugan
Faculty of Mechanical Engineering Department,
Coimbatore Institute of Tech.,
Coimbatore, Tamilnadu, India

G. Buvanasekaran
Welding Research Institute,
Tiruchirapalli, Tamilnadu, India

methodology being the traditional technique for modeling and optimization is used in most of the investigations.

Recently, Benyounis et al. [4] have presented laser butt welding of medium carbon steel which gives the effect of laser welding parameters on the heat input and weld bead profile. Mathematical models were developed to predict the heat input and weld bead profile using three level Box–Behnken design. Optimization of the keyhole parameters was done using response surface methodology [5]. Optimal solutions were found that would improve the weld quality, increase productivity and minimize the total operation cost.

Murugan and Parmar [6] have developed mathematical models to study the effect of MIG process parameters on bead geometry in surfacing of stainless steel and the direct and interaction effect of process parameters were analyzed. The authors have also studied the effect of submerged arc welding process variables on dilution and bead geometry in single wire surfacing [7].

Jeng and Mau [8] have used neural network techniques of back propagation and learning vector quantization to predict the laser welding parameters for butt joint.

Chang and Na [3] have developed a combined model of finite element analysis and neural network which can be effectively applied for the prediction of laser spot weld bead shapes of stainless steel welded with gap and without gap.

Correia et al. [9] stated that both genetic algorithms and response surface methodology were capable of locating optimum condition with relatively small number of experiments in gas metal arc welding of stainless steel.

This paper presents the mathematical models developed using response surface methodology for predicting the main and interaction effects of laser beam welding variables on bead geometry shown in Fig. 1 from the experimental data obtained for welding of AISI 304 stainless steel sheets of 2.5 mm thickness. The experiments were based on the central composite (CCD) rotatable design matrix. Regression analysis was used to develop the models and the analysis of variance method was used to test their adequacy.

2 Plan of investigation

The research work was planned to be carried out in the following steps:

1. Identifying the important process control variables;
2. Developing the design matrix;
3. Finding the upper and lower limits of the control variables;
4. Conducting the experiments as per the design matrix;
5. Recording the responses, viz. depth of penetration (PD), bead width (BW), area of penetration (AP);
6. Developing the mathematical models;
7. Calculating the co-efficient of the polynomials;
8. Checking the adequacy of the models developed;
9. Testing the significance of the regression coefficients and arriving at the final mathematical models;
10. Presenting the main effects and the significant interactions between the different parameters in graphical form;
11. Conformity test.

2.1 Identification of process variables

The independently controllable process parameters affecting the bead geometry and quality were identified as: laser beam power (BP), welding speed (WS) and laser beam incident angle (BA) which is shown in Fig. 2. The shielding gas flow rate is maintained as constant for all the trials. A tight fit-up is provided for the butt joint.

2.2 Design matrix

The response surface methodology (RSM) is used in the design matrix formation which is an empirical modelling approach using polynomials as local approximations to obtain the true input/output relationships. The most popular of the many classes of RSM designs is the CCD, which can be naturally partitioned into two subsets of points; the first subset estimates linear and two factor interaction effects while the second subset estimates curvature effects. CCD's are very efficient, providing much information on experiment variable effects and overall experimental error in a minimum number of required runs. The selected CCD matrix shown in Table 2 consists of 20 sets of coded conditions composed of a full factorial 2^3=8 plus 6 centre

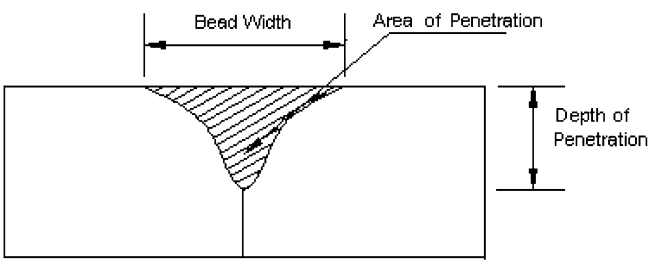

Fig. 1 Weld bead geometry

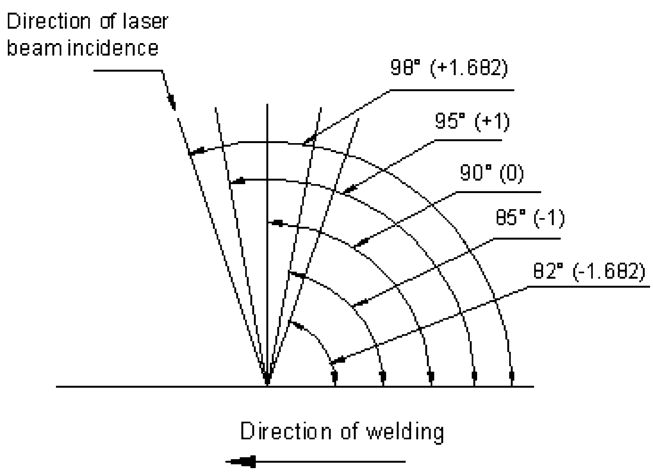

Fig. 2 Angle of Incidence of laser beam

Table 1 Control parameters and levels

Parameter	Units	Notation	Factor levels				
			−1.682	−1	0	1	1.682
Beam power	Watts	BP	580	750	1000	1250	1420
Welding speed	mm/min	WS	580	750	1000	1250	1420
Beam angle	Degrees	BA	82	85	90	95	98

points and 6 star points [10]. The star points represent the high and low value for each factor in the design.

2.3 Finding the limits of the process variables

The variables are known as natural variables if they were expressed in physical units of measurement. In the RSM, the natural variables are transformed into coded variables which are dimensionless. Trial runs were conducted by varying one of the parameters while keeping the rest at constant values. The working range was decided by visually inspecting the bead for smooth appearance. The maximum capacity of the machine is to produce 2 kW of laser power and the safer working range was identified as between 0.5 to 1.5 kW of power. The upper limit of the factor was coded as +1.682 and the lower limit as −1.682, the coded values for intermediate ranges being calculated from the relationship

$$X_i = 1.682[2X - (X_{max} + X_{min})]/[X_{max} - X_{min}], \quad (1)$$

where X_i is the required coded value of a variable X; X is any value of the variable from X_{max} to X_{min}; X_{min} is the lower level of the variable; and X_{max} is the upper level of the variable.

For example, to obtain the coded value for a beam power of 580 Watts, the minimum and maximum values being 580 Watts and 1420 Watts, substituting in Eq. 1 [3], gives a value of −1.682. (x_i=[1.682[2*580–(1420+580)]/(1420–580)]=−1.682). The selected levels of the process parameters with their units and notations are given in Table 1.

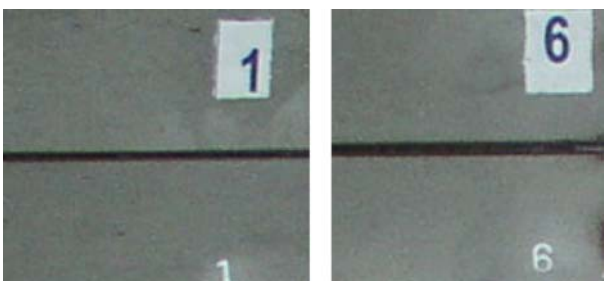

Beam Power: 580 Watts, Welding Speed: 1000 mm/min, Beam angle: 90˚

Beam Power: 1000 Watts, Welding Speed: 1000 mm/min, Beam angle: 90˚

Fig. 3 Typical laser butt welded sheets with values of the process variables

2.4 Conducting experiments as per design matrix

A 2 KW solid state Nd:YAG laser welding machine manufactured by Lumonics Ltd. England (Model MW 2000) was used to conduct the experiment. From the laser source the laser beam was sent through a fibre optic cable. The energy comes out of the fibre with a uniform power density across the fibre diameter and diverges at an angle of zero. A focusing device is used to form an image of the fibre on the work piece. Helium inert gas was supplied at the rate of 10 litres per minute to avoid contamination of the molten pool. AISI 304 Stainless steel plate of 100 × 40 × 2.5 mm size, 20 numbers of butt joints were welded by varying the process variables as per the design matrix. During the actual operation of laser welding for butt joints, the welding gap must be maintained at reasonable size to make sure that it is small enough for the laser beam not to pass straight through welding gap [8]. The specimens were prepared for tight fit-up and cleaned with acetone initially. The spot diameter of the laser beam was maintained as 0.8 mm with a focal length of 160 mm. The focused laser beam must be aligned with the centre of the joint exactly, if any misalignment occurs, then one side of the material could be completely melted and the other side partially melted. Because of this difficulty the position of laser beam was thoroughly checked by the laser CNC system and then welding was performed.

The experiments were conducted according to the design matrix at random to avoid systematic errors creeping into the system. Typical welded sheets are shown in Fig. 3 along with the values of the process variables used in the respective trial.

2.5 Recording of responses

The welded sheets were cross sectioned at their mid-points to obtain test specimens of 15 mm width. The specimens were prepared by the usual metallurgical polishing methods. The weld bead profiles were traced using an optical profile projector and the bead dimensions, viz., penetration depth (PD); bead width (BW) and area of penetration (AP) were measured with the help of a digital planimeter having an accuracy of one micron. The observed values of PD, BW, and AP are given in Table 2.

Table 2 Design matrix and observed values of bead dimensions

Sl.No	Design matrix			Bead parameters		
	BP	WS	BA	PD, mm	BW, mm	AP, mm^2
1	−1	−1	−1	0.534	0.969	7.055
2	1	−1	−1	0.967	1.453	19.58
3	−1	1	−1	0.556	1.081	8.333
4	1	1	−1	0.709	1.139	11.098
5	−1	−1	1	0.611	1.007	8.503
6	1	−1	1	1.002	1.093	17.058
7	−1	1	1	0.534	0.961	6.223
8	1	1	1	0.872	0.953	13.05
9	−1.682	0	0	0.336	0.957	4.468
10	1.682	0	0	0.903	1.000	15.783
11	0	−1.682	0	0.831	1.213	14.8
12	0	1.682	0	0.633	0.983	9.08
13	0	0	−1.682	0.728	1.139	11.655
14	0	0	1.682	0.667	1.040	8.958
15	0	0	0	0.742	0.885	10.745
16	0	0	0	0.702	1.092	11.938
17	0	0	0	0.676	1.157	12.955
18	0	0	0	0.675	1.050	10.798
19	0	0	0	0.664	1.097	9.715
20	0	0	0	0.594	1.039	8.76

BP=Beam power, WS=Welding speed, BA=Beam angle
PD=Depth of penetration, BW=Bead width, AP=Area of penetration

2.6 Development of mathematical model

The response function representing any of the weld bead dimensions can be expressed as Y=f (BP, WS, BA) where, Y= the response or yield. The second order polynomial (regression) equation used to represent the response surface for k factors is given by

$$y = b_0 + \sum_{i=1}^{k} b_i x_i + \sum_{i=1}^{k} b_{ii} x_i^2 + \sum_{i,j=1, j\neq i}^{k} b_{ij} x_i x_j, \quad (2)$$

and for three factors, the selected polynomial could be expressed as

$$Y = b_0 + b_1\,BP + b_2\,WS + b_3\,BA + b_{11}\,BP^2 + b_{22}\,WS^2 + b_{33}BA^2 + b_{12}\,BP\,WS + b_{13}BP\,BA + b_{23}WS\,BA. \quad (3)$$

2.7 Coefficients of models

The values of the coefficients of the polynomial were calculated by regression with the help of following equations [10]:

$$b_0 = 0.1666 \sum (Y) - 0.0568 \sum (X_{ii}\,Y) \quad (4)$$

$$b_i = 0.0732 \sum (X_i Y) \quad (5)$$

$$b_{ii} = 0.0625 \sum (X_{ii} Y) + 0.00689 \sum (X_{ii} Y) - 0.0568(Y) \quad (6)$$

$$b_{ij} = 0.1250 \sum (X_{ij}\,Y). \quad (7)$$

A Systat software package was used to calculate the values of these coefficients for different responses.

2.8 Assessing adequacy of developed models

The adequacies of the models were tested using the analysis of variance technique (ANOVA). According to this technique, if the calculated value of the F-ratio of the model exceeds the standard tabulated value of the F-ratio for a desired level of confidence (say 95%), then the model may be considered adequate within the confidence limit. Table 3 shows that all the models were adequate.

2.9 Testing coefficients for significance

The value of the regression coefficients gives an idea of the extent to which the control variables quantitatively affect the responses. The less significant coefficients can be eliminated with their associated responses in order to avoid cumbersome mathematical labor. The student's t test [11] was used to determine significant coefficients. According to this test, when the calculated value of t, corresponding to the coefficient, exceeds the standard tabulated value for a desired level of probability (say 95%), the coefficient becomes significant. The final models were developed

Table 3 Analysis of variance for testing adequacy of models

Bead Parameters	Sum of squares		Degrees of freedom		F-ratio	Remarks
	regression	residual	regression	residual		
Penetration depth	0.448	0.041	5	14	30.916	Adequate
Bead width	0.186	0.101	5	14	5.148	Adequate
Penetration area	243.110	22.879	5	14	29.753	Adequate

F-ratio$_{(5,14,0.05)}$=4.64

Table 4 Comparison of squared multiple R values, adjusted square multiple R and standard error of estimate for full and reduced models

Response	Squared multiple, R		Adjusted square multiple R		Standard error of estimate	
	Full model	Reduced model	Full model	Reduced model	Full model	Reduced model
PD	0.935	0.917	0.879	0.888	0.056	0.054
BW	0.715	0.648	0.458	0.522	0.090	0.085
AP	0.915	0.914	0.839	0.883	1.500	1.278

using only these significant coefficients. The squared multiple R values and standard error of estimate of the full models and the reduced models are presented in Table 4 which shows that the reduced models are better than the full models. The adjusted square multiple R-values are improved for reduced models.

2.10 Final models

The final mathematical models determined by the above analysis are represented below both in coded and natural form. To find the bead geometry (output response), the input parameters of beam power, welding speed and beam angle are to be substituted in coded value for the mathematical equation in coded form (Eqs. 8, 9, 10). Actual values of beam power, welding speed and beam angle are to be substituted in the mathematical equation in natural form (Eqs. 11, 12, 13). Either coded form or natural form can be used to find the bead geometry. Calculations are simplified by coding. The range of parameters in actual units are simplified between the limits of −1.682 and +1.682 which are dimensionless.

CODED FORM

$$\begin{aligned}\text{Depth of Penetration, } DP = {} & 0.677738 + 0.166104\ BP - 0.056818\ WS + 0.011012\ BA + 0.027913\ WS \\ & WS - 0.041625\ BP\ WS\end{aligned} \tag{8}$$

$$\begin{aligned}\text{Bead Width, } BW = {} & 1.065400 + 0.050689\ BP - 0.056732\ WS - 0.058171\ BA - 0.065000\ BP \\ & WS - 0.058000\ BP\ BA\end{aligned} \tag{9}$$

$$\begin{aligned}\text{Area of Penetration, } AP = {} & 1.0663058 + 3.639107\ BP - 1.692240\ WS - 0.422335\ BA - 0.534024\ WS \\ & WS - 1.436000\ BP\ WS\end{aligned} \tag{10}$$

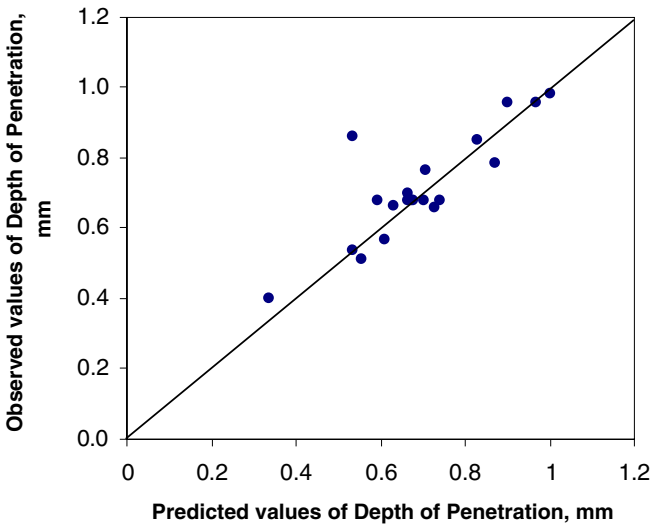

Fig. 4 Scatter diagram for depth of penetration

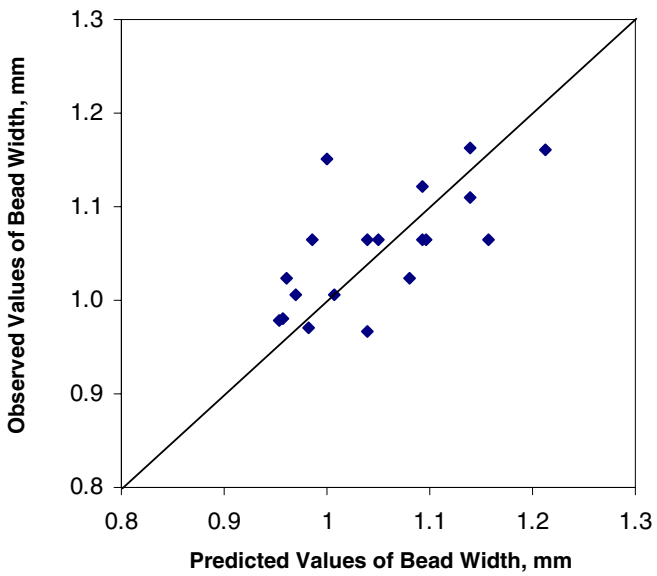

Fig. 5 Scatter diagram for bead width

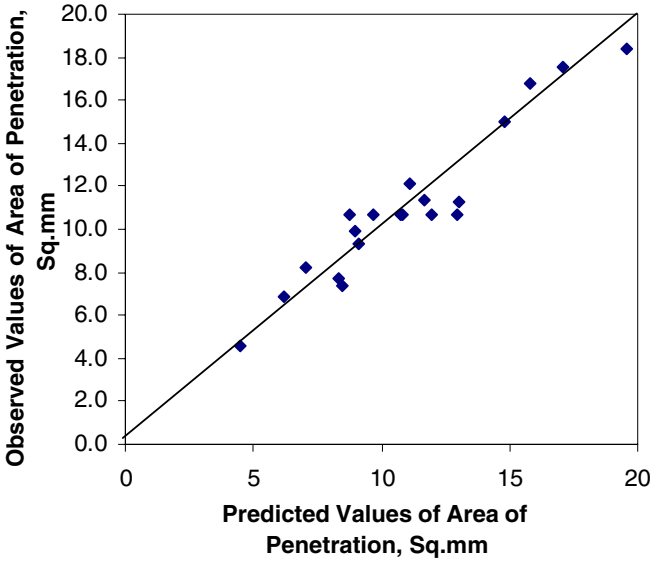

Fig. 6 Scatter diagram for area of penetration

NATURAL FORM

$$\text{Depth of Penetration, } DP = -0.19101301 + 0.0013374\,BP - 0.00045707\,WS + 0.00236890\,BA + 0.00000045\,WS - 0.00000067\,BP\,WS \quad (11)$$

$$\text{Bead Width, } BW = -3.04761220 + 0.00541893\,BP + 0.0081298\,WS + 0.03441220\,BA - 0.00000104\,BP - 0.00004640\,BP\,BA \quad (12)$$

$$\text{Area of Penetration, } AP = -3.93017986 + 0.03754014\,BP - 0.00092556\,WS - 0.08456098\,BA + 0.00000856\,WS - 0.00002298\,BP\,WS \quad (13)$$

The validity of the above equations can be known from Figs. 4, 5, 6, which show the relationship between the measured and computed values of PD, BW and AP, respectively. These scatter diagrams indicate that the above equations show a good relationship between the measured and computed values of PD, BW and AP.

2.11 Conformity test

To determine the accuracy of the mathematical models, conformity test runs were conducted after the development of the models using the same experimental setup. The process variables were assigned intermediate values other than that used in the design matrix and the conformity test runs were carried out. The responses were measured and compared with the predicted values of bead parameters that are given in Table 5. The results show that models are accurate.

3 Results

The mathematical models can be employed to predict the geometry of the weld bead for the range of parameters used in the investigation by substituting their respective values in coded form. Based on these models, the main and interaction effects of the process parameters on bead geometry were computed and plotted. It is also possible to obtain values for the control factors by substituting the values of the desired bead geometry in coded form.

4 Discussion

The main effects of the different laser beam welding process variables on the weld bead geometry predicted from the mathematical models are presented in Figs. 7, 8, 9, showing the general trends between cause and effect.

Table 5 Comparison of actual and predicted values of bead parameters

Sl.no	Process parameters in coded form			Actual values of bead parameters			Predicted values of bead parameters			Error, %*		
	BP	WS	BA	PD	BW	AP	PD	BW	AP	PD	BW	AP
1	+0.400	−1.201	−1.682	0.898	1.294	16.940	0.854	1.322	16.322	5.133	−2.111	3.789
2	−0.400	+0.400	−1.682	0.605	1.061	9.713	0.581	1.092	9.556	4.099	2.808	1.642
3	−1.602	−1.201	+1.682	0.482	0.943	4.368	0.459	0.986	4.163	5.108	4.333	4.934
3	+0.801	+1.201	+1.682	0.718	0.758	10.115	0.761	0.799	9.801	−5.686	5.173	3.202

*error, %=[(actual value – predicted value) / predicted value] * 100

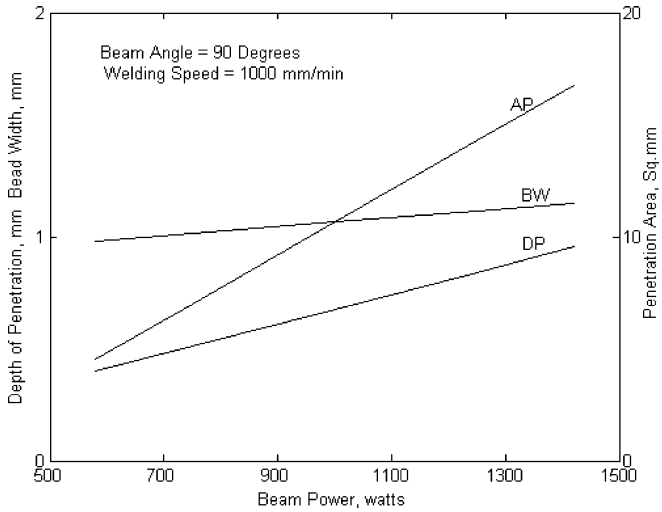

Fig. 7 Direct effect of beam power on bead geometry

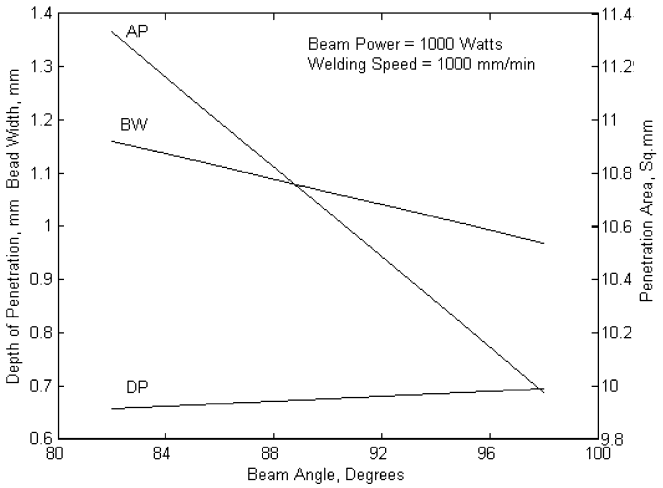

Fig. 9 Direct effect of beam angle on bead geometry

4.1 Direct effects of process parameters

Figure 7 shows the direct effect of beam power on bead geometry. As the magnitude of laser power is increased from 580 to 1420 W, the output responses of depth of penetration, bead width and area of penetration are found to increase. This is due to the increase in heat input when beam power increases resulting in more melting of base material. The variation in bead width is less significant for the variation of beam power [12] indicating that it may be a function of laser beam spot diameter. As the spot diameter was maintained constant for all the trials, not much of variation was observed in bead width.

Figure 8 shows the direct effect of welding speed on bead geometry. It is seen that as the welding speed increases depth of penetration, bead width and area of penetration decreases, because of time of exposure of laser energy on the workpiece decreases. At the higher range of welding speed, depth of penetration and area of penetration are found to increase. This may be due to the effect of keyholing is predominant for these range of welding speed.

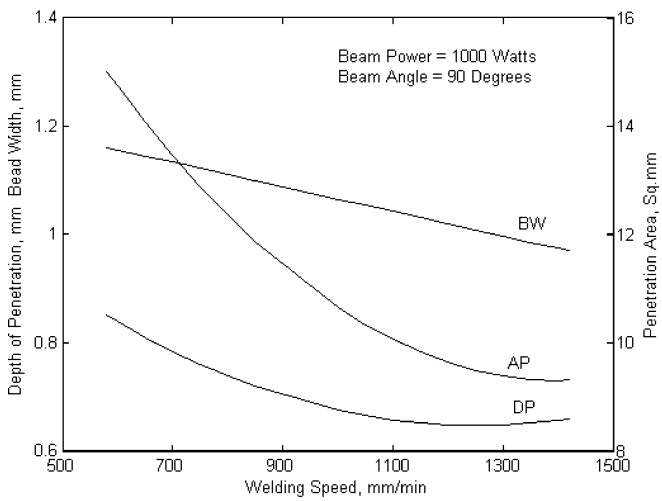

Fig. 8 Direct effect of welding speed on bead geometry

At high welding speed, attenuation of beam energy by plasma is less significant. This results in more exposure of laser beam on the sample surface.

Figure 9 shows the direct effect of beam angle on bead geometry. Generally the laser beam is not positioned perpendicular to the workpiece, for the main reason that the reflected laser energy may impair the optic system, which is costly. Hence a small angular tilt is given to the laser beam. The beam incident angle is varied with reference to the positive x-axis. The welding operation is done from the right to left hand side (left wards technique). It is evident that as beam angle increases from 82 to 98 deg anti clockwise bead width and area of penetration decreases and the depth of penetration increases minimally. Since the beam is pointed in the direction of the welding, it preheats the edges of the joint at 82 deg beam angle, as the beam angle is changed in direction the coupling of laser beam to material decreases and hence the responses are decreasing.

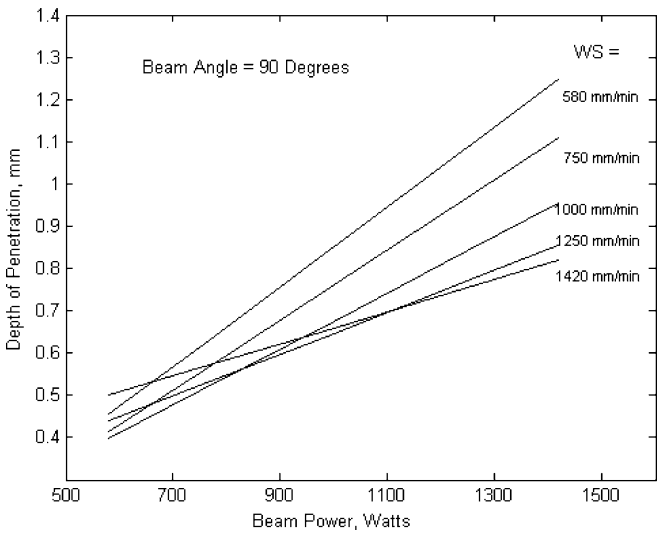

Fig. 10 Interaction effect of beam power and welding speed on depth of penetration

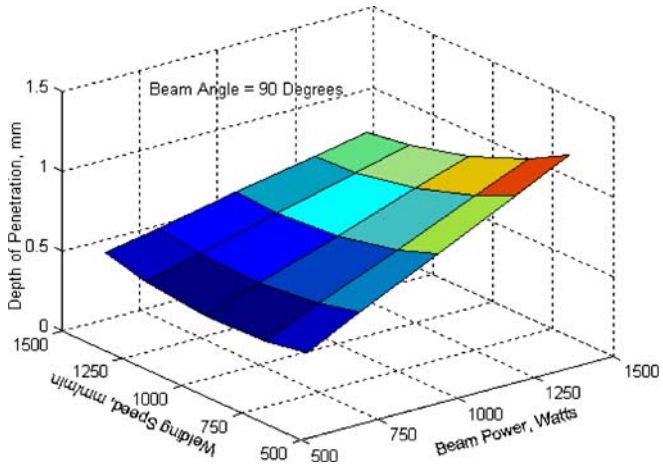

Fig. 11 Interaction effect of beam power and welding speed on depth of penetration – surface graph

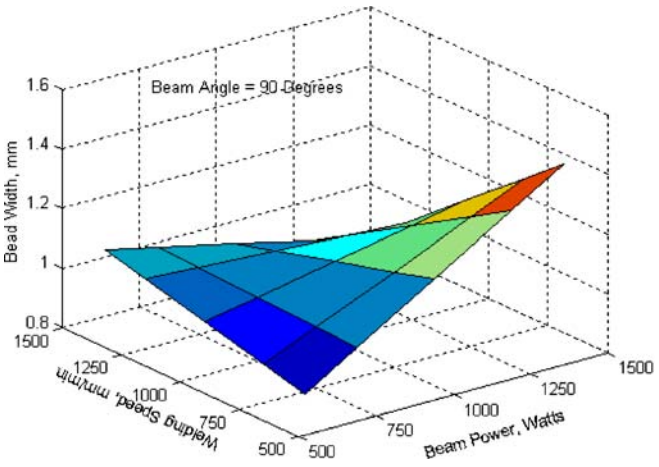

Fig. 13 Interaction effect of beam power and welding speed on bead width – surface graph

4.2 Interaction effects of process parameters

Figures 10 and 11 show the interaction effects of beam power and welding speed on depth of penetration. As the beam power is increasing from minimum to maximum the depth of penetration is found to increase and as welding speed is increasing the depth of penetration decreases.

Figures 12 and 13 depict the interaction effect of beam power and welding speed on bead width. Bead width increases with the increase in beam power when welding speed increases from 580 to 1000 mm/min. When welding speed is more than 1000 mm/min, bead width decreases with the increase in beam power. This may be due to the effect of welding speed on width is more than the effect of power on width.

Figures 14 and 15 depict the interaction effect of beam power and beam angle on bead width. Bead width increases with the increase in beam power when beam angle increases from 82 to 90 degrees. When beam angle is more than 90 degrees, bead width decreases with the increase in beam power.

Figures 16 and 17 show the interaction effect of beam power and welding speed on area of penetration.

5 Conclusion

The conclusions arrived at from the above investigations are:

1. A five level factorial technique can be employed easily for developing mathematical models for predicting weld bead geometry in the laser welding process which can be used effectively in analyzing the cause and effect of the process parameters on response.
2. Depth of penetration, bead width and area of penetration increases with an increase of beam power and decreases with an increase in beam angle.

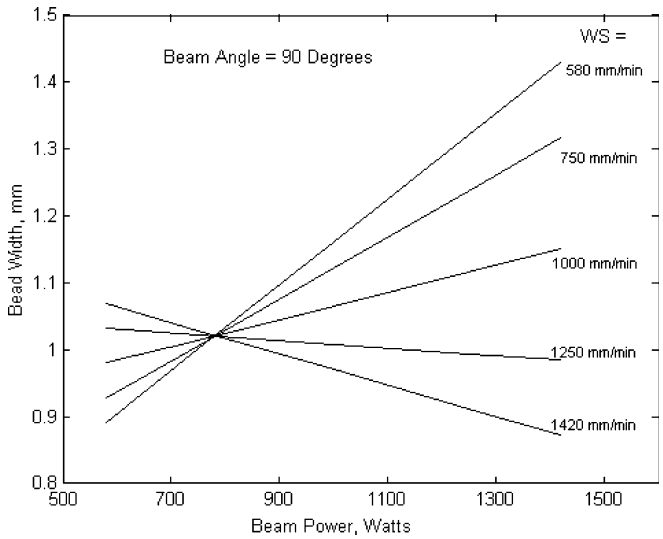

Fig. 12 Interaction effect of beam power and welding speed on bead width

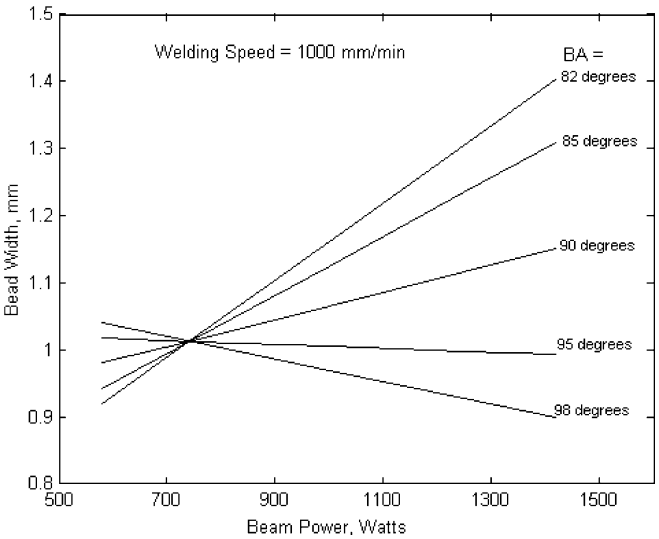

Fig. 14 Interaction effect of beam power and beam angle on bead width

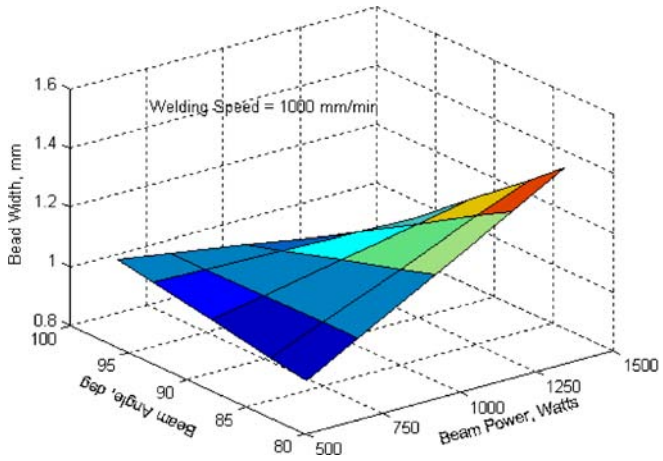

Fig. 15 Interaction effect of beam power and beam angle on bead width – surface graph

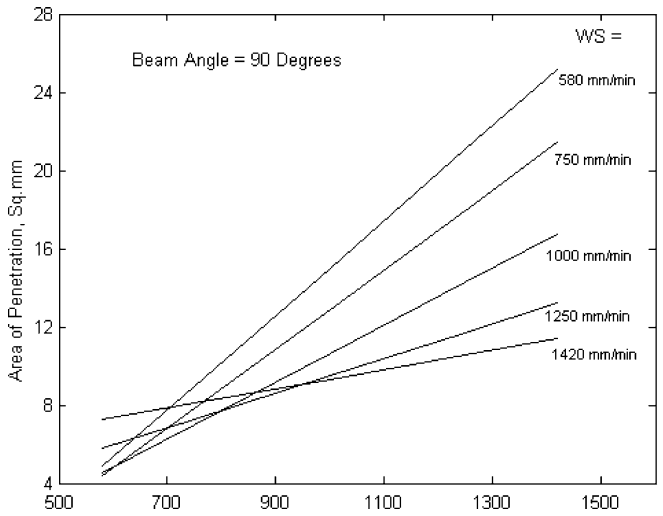

Fig. 16 Interaction effect of beam power and welding speed on area of penetration

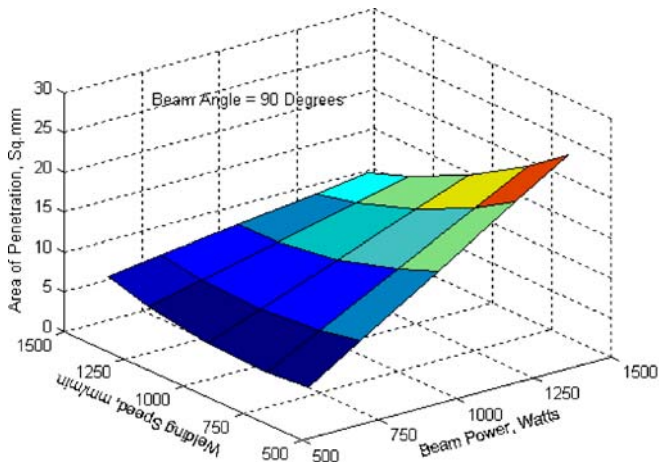

Fig. 17 Interaction effect of beam power and welding speed on area of penetration – surface graph

3. Depth of penetration, bead width and area of penetration decreases with an increase of welding speed, and at higher welding speed depth of penetration and area of penetration increases slightly due to keyholing.
4. It is found that the variation in bead width is very minimum and not so significantly affected by the parameters of beam power, welding speed and beam angle.
5. The three dimensional surface graphs clearly show the interactive effects of various input parameters considered on the bead geometry.

Acknowledgements The authors wish to thank Welding Research Institute, Trichy for providing the facilities for conducting trials. They also wish to thank the management of Coimbatore Institute of Technology and Government College of Technology, Coimbatore for having provided all the necessary facilities for the completion of the work.

References

1. Steen WM (1991) Laser material processing. Springer, Berlin Heidelberg New York
2. Dawes C (1992) Laser welding. Abington, New York
3. Chang WS, Na SJ (2001) Prediction of laser spot weld shape by numerical analysis and neural network. Metallurgical Mater Trans 32(B):723–731
4. Benyounis KY, Olabi AG, Hashmi MSJ (2005) Effect of laser welding parameters on the heat input and weld bead profile. J Mater Process Technol pp 978–985
5. Benyounis KY, Olabi AG, Hashmi MSJ (2005) Optimizing the laser welded butt joints of medium carbon steel using RSM. J Mater Process Technol pp 986–989
6. Murugan N, Parmar RS (1994) Effect of MIG process parameters on the geometry of the bead in the automatic surfacing of stainless steel. J Mater Process Technol 41:381–398
7. Murugan N, Parmar RS, Sud SK (1993) Effect of submerged arc process variables on dilution and bead geometry in single wire surfacing. J Mater Process Technol 37:767–780
8. Jeng J-Y, Mau T-F (2000) Prediction of laser butt joint welding parameters using back propagation and learning vector quantization networks. J Mater Process Technol pp 207−218
9. Correia DS, Goncalves CV, da Cunha SS, Ferraresi VA (2005) Comparison between genetic algorithms and response surface methodology in GMAW welding optimization. J Mater Process Technol 160:70–76
10. Cochran WG, Cox GM (1963) Experimental designs. Asia Pub House, Bombay
11. Marimuthu K, Murugan N (2003) Prediction and optimization of weld bead geometry of plasma transferred arc hard faced valve seat wires. Surface Eng J 19:143–149
12. Leonard M (1996) Laser material processing. Dekker, New York